Subtidal Response of Scotian Shelf Circulation to Local and Remote Forcing. Part I: Observations

FRANKLIN B. SCHWING

Department of Oceanography, Dalhousie University, Halifax, Nova Scotia, Canada

(Manuscript received 29 August 1990, in final form 26 August 1991)

ABSTRACT

Data collected during the Canadian Atlantic Storms Program (CASP) suggest that two primary current regimes exist on the Scotian Shelf during winter. Moorings inside the 100-m isobath feature currents that are parallel to the general bathymetry and have small eastward mean velocities. The time-varying part of the flow is nearly rectilinear alongshelf at typical maximum velocities of 0.2–0.3 m s^{-1} and oscillates on 2–5-day periods in response to meteorological forcing. The current at locations beyond the 100-m isobath exhibits a persistent westward flow of about 0.3 m s^{-1}, denoting the dominance of the Nova Scotian Current, although smaller magnitude along- and cross-shelf fluctuations occur at synoptic frequencies. Flow in both regions is largely uniform with depth at this time of year.

The velocity response to local and remote sources of forcing was examined using a frequency (ω)-dependent multiple regression model. Flow is dominated by nonlocal forcing at $\omega < 0.2$ cpd; alongshelf wind stress is the principal local influence at low frequencies. Remote forcing is less important at higher frequencies, while the role of local cross-shelf wind stress is greater. The effect of local wind forcing is generally small and varies substantially on horizontal scales of order 10 km. Current typically lags wind stress by about 30°–45° at $\omega < 0.5$ cpd; the response to alongshelf wind stress also suggests a phase propagation to the west. The typical response to alongshelf wind forcing is consistent with previous quasi-steady observations and model results from the Scotian Shelf. The contribution of cross-shelf wind stress is limited to a near-surface flux in the synoptic band. The remote response decreases offshore and to the west and propagates westward, in the direction that coastally trapped waves propagate. The current response to local and remote forcing is uniform with depth at nearly all locations. Local and remote contributions to alongshelf velocity, integrated across the mooring array, are in geostrophic balance with the cross-shelf subsurface pressure (SSP) gradient. Together, the two wind stress components and a SSP record representing nonlocal forcing explain 40%–80% of alongshelf flow, compared to 95% of the SSP signal.

Some of the large-scale flow features are consistent with variations seen in SSP data. The most obvious similarity is the remotely forced response. However, these results also reveal substantial variations in the current on scales of 10–100 km that are not reflected in the SSP field. Irregular shelf bathymetry is thought to induce the observed variations in circulation. This study also demonstrates the need to include remote forcing effects, in the form of a properly prescribed backward boundary condition, in shelf circulation models.

1. Introduction

The Scotian Shelf region off eastern Canada lies in the path of numerous winter cyclones, due to its location relative to continental land masses and the distribution of upper-atmospheric circulation patterns. The track, direction, and intensity of these storms are variable. In general, the storms are quite severe, featuring extremely low central pressures, high winds, and intense precipitation (cf. Lewis and Moran 1984). Like most midlatitude continental shelves, meteorological forcing is an important source of energy to Scotian Shelf dynamics at 2–10-day periods (Petrie and Smith 1977; Smith et al. 1978; Sandstrom 1980; Schwing 1989). The Canadian Atlantic Storms Program (CASP), formulated to study the nature of East Coast winter storms (Stewart et al. 1987) and coordinated with the Genesis of Atlantic Lows Experiment (GALE) along the eastern United States, included an intensive oceanographic field sampling program to examine how winter storms drive circulation on the inner Scotian Shelf (Anderson et al. 1989; Anderson and Smith 1989).

Previous analysis of the subinertial, meteorologically driven response of subsurface pressure (SSP) during CASP has provided considerable insight to the Scotian Shelf dynamics (Schwing 1989). Schwing found that subinertial variations in SSP are highly coherent throughout the Scotian Shelf region, and well correlated to fluctuations in wind stress forcing over the shelf. A multiple regression model showed that alongshelf stress is the primary source of local meteorological forcing, although nonlocally generated motions, as approxi-

Corresponding author address: Dr. Franklin B. Schwing, National Marine Fisheries Service/NOAA, Pacific Fisheries Environmental Group, Southwest Fisheries Science Center, P.O. Box 831, Monterey, CA 93942.

mated by Louisbourg SSP at the eastern end of the province (Fig. 1), are also important. Wind stress and nonlocal forcing combine to explain over 90% of SSP variance at subinertial frequencies.

Schwing (1989) also concluded that the amplitude of the SSP response to local wind forcing increases from east to west. The phase of the response also propagates to the west. Time-dependent solutions to a simple, frictional numerical model that features spatially uniform alongshelf wind-stress forcing and idealized bathymetry closely resemble the observed wind-forced response, as well as the pattern found by Csanady (1978) for the steady arrested topographic wave model, and suggest that the quasi-steady limitations imposed by the long-wave and rigid-lid approximations are valid for explaining SSP variations at synoptic and lower frequencies. The amplitude and phase of the nonlocal response were found to be consistent with frictional coastally trapped wave (CTW) theory, the most direct evidence of shelf wave activity on the Scotian Shelf to date.

The SSP signals are related to transport through the equations of motion and continuity, and can be considered to be integral measures of the circulation regime (cf. Rhines 1977, pp. 196–202). Because of this, we may expect the large-scale SSP and current responses to meteorological forcing to be complementary. Thus, the interpretation of the SSP results in Schwing (1989) can be verified by an examination of the CASP current meter records, and vice versa.

However, density stratification and mesoscale variations in bathymetry or the forcing field may induce variations in the current on small vertical and horizontal scales. Because sea level integrates depth-dependent current variability, vertical differences in velocity are "smoothed over" in SSP observations. Similarly, flow over highly irregular bathymetry, or forced by a spatially complex wind stress, will feature smaller horizontal length scales than will SSP (Willebrand et al. 1980). As Rhines (1977) observed regarding the relationship between pressure and its derivative velocity, "Integration smooths, differentiation roughens." Therefore, SSP is likely to be more coherent with large-scale forcing than is the current. Spatial coherence scales within the current field are also probably smaller.

It also has been suggested that the barotropic modal structure of remote, or free, energy in currents is different from that in SSP (Hsieh 1982). Hsieh notes that velocity observations reflect the structure of the free response more accurately, since SSP data are strongly biased for the lowest mode, and because "the ratio of potential to horizontal kinetic energy is . . . very small for shelf waves." Thus, while similar patterns in the response of each may verify the importance of certain

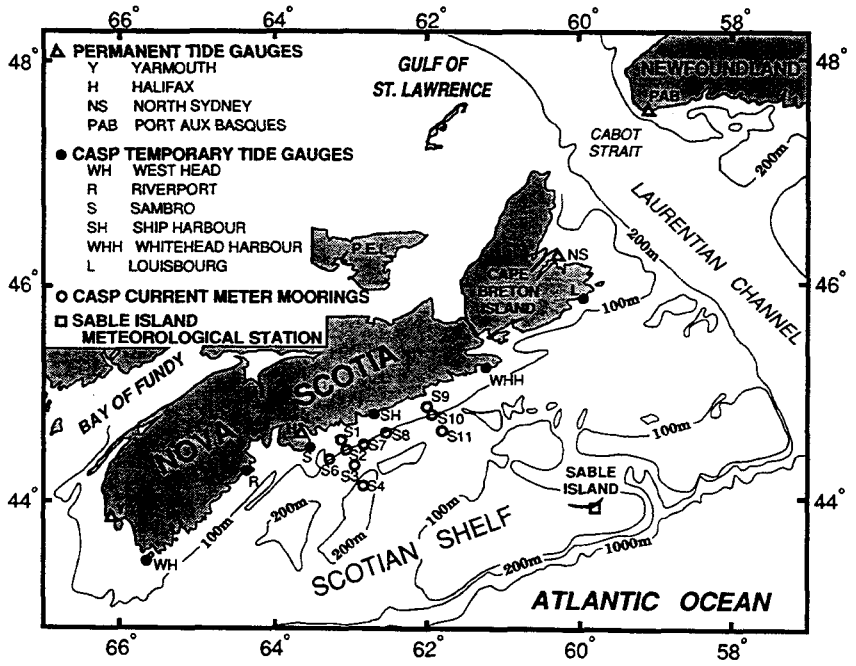

FIG. 1. Location map showing positions of CASP current meter moorings and coastal subsurface pressure stations. Wind data obtained at Sable Island AES meteorological station.

dynamical processes, it cannot be assumed that the response of the current regime will be identical to that of the SSP field. An analysis of SSP provides only a foundation of the dynamics; current observations allow mesoscale and baroclinic circulation features to be defined.

In this study, the response of the subinertial circulation on the Scotian Shelf to local and remote forcing is described and interpreted, using statistical techniques applied previously to SSP observations (Schwing 1989). Results are compared to those from the SSP analysis to confirm the conclusions of that investigation. In particular, the behavior of the current response to nonlocal forcing may verify the existence of CTWs on the Scotian Shelf, as suggested by the SSP results. The current response also provides information on mesoscale variations that are otherwise covered up by the integrated response of the pressure field. The potential importance of baroclinic motions, which cannot be discerned from SSP data, can be determined as well. The observed current response described here is compared to numerical model results in a companion paper (Schwing 1992).

In section 2, the morphology of the Scotian Shelf is briefly described, since it may contribute to variations in the velocity field. The circulation observed during CASP is described in section 3 and compared to wind stress and SSP in time series and spectral formats. A frequency-dependent regression analysis of the current response to local and remote forcing is applied in section 4, and the role of each forcing term is evaluated. Section 5 provides a discussion of these results, relating them to SSP results from Schwing (1989), to other regional studies, and to existing and potential dynamical models that may be effective in explaining circulation patterns on the Scotian Shelf.

2. Physical setting

The Scotian Shelf lies offshore from Nova Scotia in a south-southeasterly direction (Fig. 1). Its length is about 700 km, while its width, as defined by the 200-m isobath at the shelf break, varies from ~250 km at its eastern end to ~150 km to the west. The coastline is generally straight, with periodic headlands and bays having topographic scales O(10–20 km). Nearshore isobaths (<100-m depth) follow the trend and variations of the coastline. However, much of the shelf's bathymetry is highly irregular, particularly over the eastern portion of the shelf. At distances greater than ~40 km from the coast, the typical depth of 100–150 m is interrupted by several bathymetric anomalies of glacial origin, including basins featuring depths of more than 200 m and banks that shoal to 50 m and less. These have typical horizontal length scales O(50–100 km). Unlike the continuous continental shelf off the eastern United States, the Scotian Shelf is bathymetrically isolated, by deep channels, from the Grand Banks to the east and Georges Bank to the west. The eastern boundary of the shelf is defined by the Laurentian Channel, with a typical width of ~100 km and depth of ~400 m. The smaller Northeast Channel, west of the Scotian Shelf, extends into the Gulf of Maine toward the Bay of Fundy.

The abrupt changes in Scotian Shelf bathymetry and its relative isolation from regions to the east and west suggest the existence of a complex circulation for this shelf. Irregular bathymetry is likely to affect the flow in several ways. The importance of direct wind forcing over the Scotian Shelf will vary greatly, from dominant over the strongly frictional shallow regions to nearly negligible over the deep basins. Distantly forced propagating motions (i.e., CTWs) no longer have a smooth, continuous wave guide (Wilkin and Chapman 1987). Combined with the large changes in depth associated with bathymetric features on and adjacent to the shelf, it is possible that such propagations are scattered and dissipated on small spatial scales, as postulated by Wilkin and Chapman (1987) and others. If this effect is very strong near the source of such motions, then nonlocal forcing may have only a minor influence on the Scotian Shelf circulation. Alternatively, local scattering could result in enhanced small-scale variability in the circulation. Irregular bathymetry may also act to steer flow along isobaths (Wright et al. 1986), and even produce variability in the circulation in association with, and on the horizontal scales of, bathymetric features (Haidvogel and Brink 1986). These factors will be examined using a numerical model featuring realistic bathymetry (Schwing 1992), and should be kept in mind regarding the observations described below.

3. Observations

a. Methods

Current meter data described here were collected at ten moorings deployed on the Scotian Shelf from November 1985 to April 1986 as part of the CASP field experiment (Figs. 1 and 2). The moorings were arranged into two cross-shelf lines near Halifax (S1–S4) and Liscomb (S9–S11), and an alongshelf line situated on the 100-m isobath (S2, S6–S8, S10). The maximum extent of the array, approximately 65 km offshore and 120 km in the alongshelf direction, and close spacing of the moorings allowed mesoscale variations in the current field of order 10–100 km to be detected.

All velocity data were collected with Aanderaa RCM4S recording current meters, with a threshold of 1.5 cm s^{-1} and an accuracy of ± 1 cm s^{-1} and $\pm 5°$ in speed and direction for a velocity range of 5–100 cm s^{-1}. A total of 28 current meters (out of 34 deployed) provided sufficiently long time series of quality data to be analyzed using the spectral techniques described below. Current velocities were rotated into

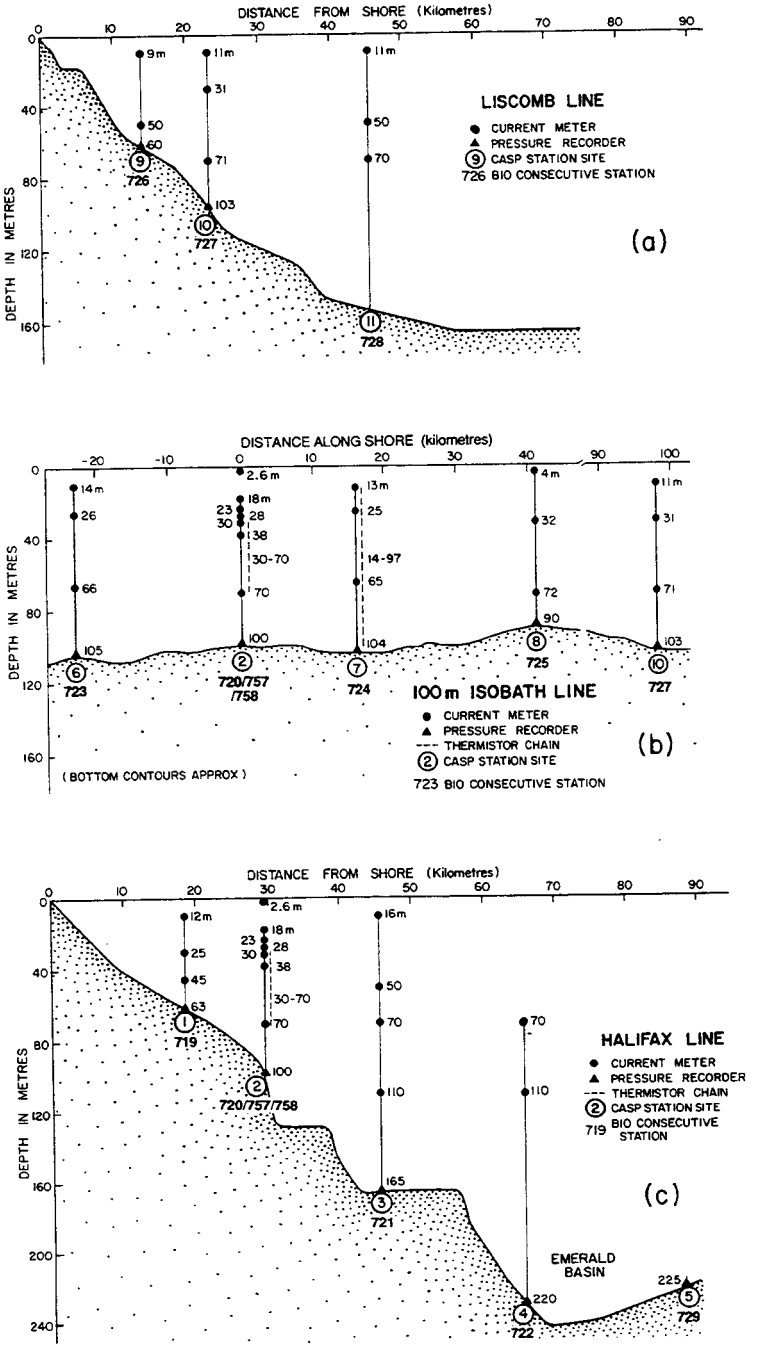

FIG. 2. Profile of (a) Liscomb current meter mooring line, (b) 100-m isobath current meter mooring line, and (c) Halifax current meter mooring line.

alongshelf ($+v = 68°$T) and cross-shelf ($+u = 158°$T) components, based on the typical coastline orientation. The principal axes of variation for most current time series were very similar to the alongshelf coordinate (Anderson and Smith 1989). Components were then low-pass filtered with a 129-weight Cartwright filter [0.036 cph (28 h) quarter-power cutoff] to remove tidal and inertial energy, and resampled at 6-hourly intervals. The bulk of the results refer to observations from the 100-m isobath moorings (Fig. 2b) as an indicator of alongshelf trends, and the Halifax line (Fig. 2c) for variability across the shelf.

Wind observations from the Sable Island Atmospheric Environmental Service (AES) station were chosen to represent meteorological conditions over the Scotian Shelf (Petrie and Smith 1977). Alongshelf (τ^y) and cross-shelf (τ^x) wind stress components were estimated at 1-h intervals from wind speed and direction, using the quadratic stress law with a variable drag coefficient (Smith and Banke 1975). The wind stress series were filtered and resampled in the same manner as the current series. For further information on the CASP deployment and data collection and processing, refer to Lively (1988) and Anderson and Smith (1989).

Power spectra for all series were calculated according to Carter and Ferrie (1979). The 32 frequency bands each had a bandwidth of 0.0625 cycles per day (cpd). Spectral results were averaged over $n = 14$ blocks of data with 50% overlap, giving $\nu = 22.9$ effective degrees of freedom (Garrett and Toulany 1982).

b. *Time series*

Low-passed current meter time series define two distinct circulation regimes on the inner portion of the Scotian Shelf (Fig. 3). Stations inside the 100-m isobath, represented by S1, typically featured a current parallel to the general bathymetry (Fig. 3a). Although the means of these records are small and typically to the east (Anderson and Smith 1989), the time-varying current was nearly rectilinear and oscillated between eastward and westward flow at periods on the order of 2–5 days. A visual comparison with Sable Island wind stress indicates a close correspondence of wind, current, and SSP events. Maximum velocities were 0.2–0.3 m s^{-1}.

The current beyond the 100-m isobath exhibited a persistent alongshelf flow to the west with average values of 0.3 m s^{-1} in the surface layer (Figs. 3c,d). These velocities suggest that the Nova Scotian Current dominates the flow outside the 100-m isobath (Drinkwater et al. 1979; Anderson and Smith 1989), although the geostrophic transports estimated by Drinkwater et al. (1979) from the baroclinic field are approximately half as large as those observed during CASP (Anderson and Smith 1989). Cross-shelf variations in flow, as well as changes in the magnitude of the alongshelf current, occurred at 2–5-day periods, again suggesting a possible meteorological response. However, the amplitudes of such variations were much smaller than those observed in shallower water.

Moorings near the 100-m isobath, typified by S2 (Fig. 3b), experienced the net westward flow seen farther offshore, as well as alongshelf current reversals that suggest the wind-forced response of the nearshore region. Time series (Fig. 3) and progressive vector plots (Fig. 4) of near-surface instruments at S1–S3 clearly demonstrate these trends; S2 and S3 exhibit the same general pattern. However, the cumulative displacement was much greater at S3. Higher-frequency oscillations, presumably associated with the passage of atmospheric pressure systems, dominate the flow at S1, and are more evident at S2 than at S3.

A comparison of instruments on a single mooring suggests the flow is essentially uniform with depth (Fig. 3). The water column closer to shore ($h < 50$ m) is well mixed (Fig. 5), presumably by a combination of surface and bottom stress. Some reduction in velocity with depth occurred in the outer region of the array. The historical position of the February front (defined by the $\sigma_t = 25.5$ isopleth) runs through S3 and S4 at about 30–50-m depth, intercepting the bottom near the 100-m isobath (Drinkwater and Taylor 1982). Hydrographic observations at the beginning and end of the CASP field experiment indicated a similar structure (Fig. 5). Thus, some baroclinically controlled events may occur in deeper water, as suggested by the S3 time series (Fig. 3c).

However, the fact that velocities observed during CASP were substantially larger than the geostrophic currents estimated from historical density measurements by Drinkwater et al. (1979) suggests that the circulation beyond the 100-m isobath was predominantly barotropic, particularly in the upper 50–100 m (Anderson and Smith 1989). Water mass properties (temperature, salinity, and density) measured at each mooring (Lively 1988), as well as hydrographic surveys conducted at the beginning and end of the field experiment (Fig. 5), verified that baroclinic processes were minimal near the surface and throughout the inner portion of the array, but may have influenced the circulation in deeper areas of the shelf. More important, density variations at synoptic (<10 d) periods were small relative to longer-period fluctuations (Lively 1988). The density field changed relatively little over the course of the experiment (Fig. 5). Thus, the baroclinic contribution can be thought of as a relatively constant background flow added to the higher-frequency (barotropic) fluctuations of interest in this study.

A visual examination of the alongshelf current field suggests that coherence length scales are quite large in the nearshore (S1 vs S9) region of the Scotian Shelf but reduced farther offshore (S3 vs S11) (Fig. 6a). Some variation appears along the 100-m isobath (Fig. 6b). Most subinertial events were observed throughout

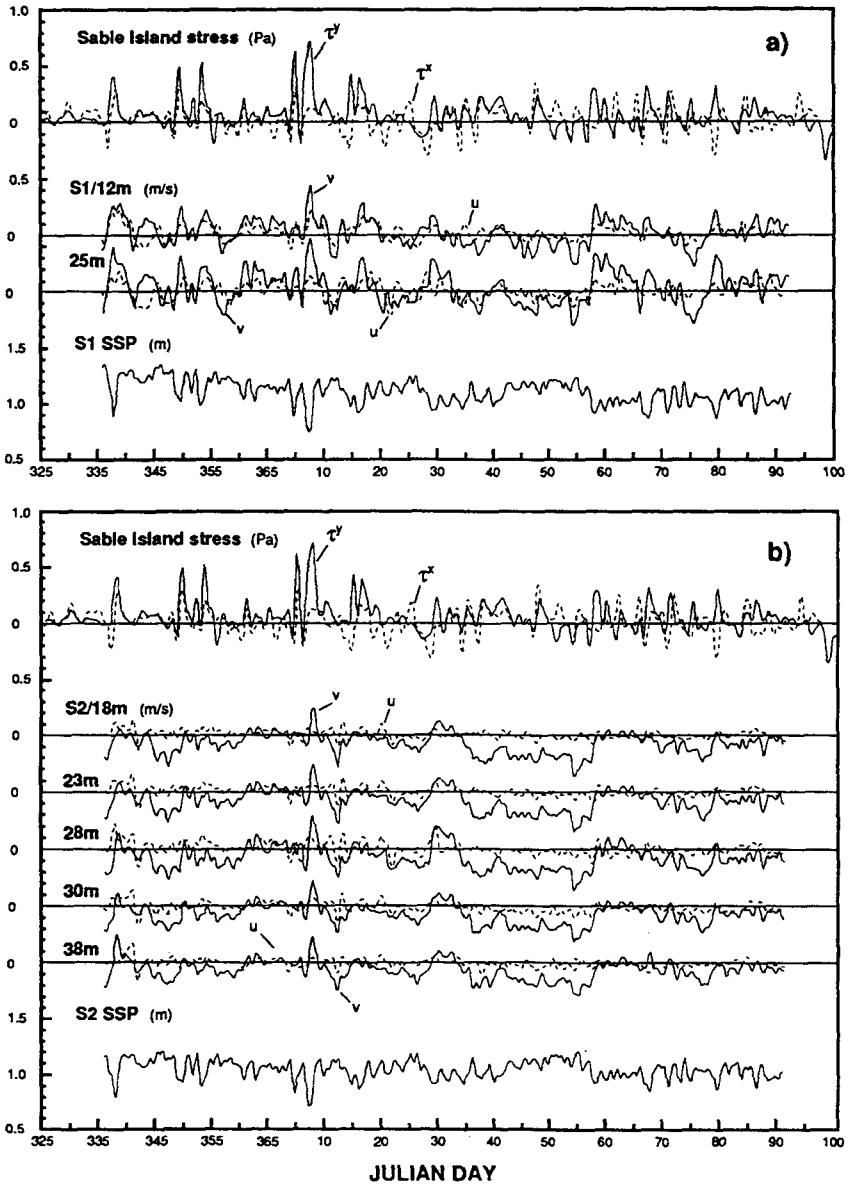

FIG. 3. Low-pass filtered time series of current meter components at (a) S1, (b) S2, (c) S3, and (d) S4. Solid line denotes alongshelf (v) component, positive to east. Broken line denotes cross-shelf (u) component, positive offshore. Low-passed bottom pressure, alongshelf (τ^y), and cross-shelf (τ^x) Sable Island wind stress

the array. However, substantial differences in the magnitude and direction of flow during individual events occurred on scales as small as 10 km. Alongshelf velocity time series are generally correlated at the significant frequencies discussed below, but no clear pattern is apparent that allows coherence length scales to be quantified.

c. *Power spectra*

The presentation of low-passed current power spectra in variance-preserving form reflects the relationship between wind stress, current, and bottom pressure at locations inside the 100-m isobath (Fig. 7). The variance distribution of Sable Island wind stress (Fig. 7a)

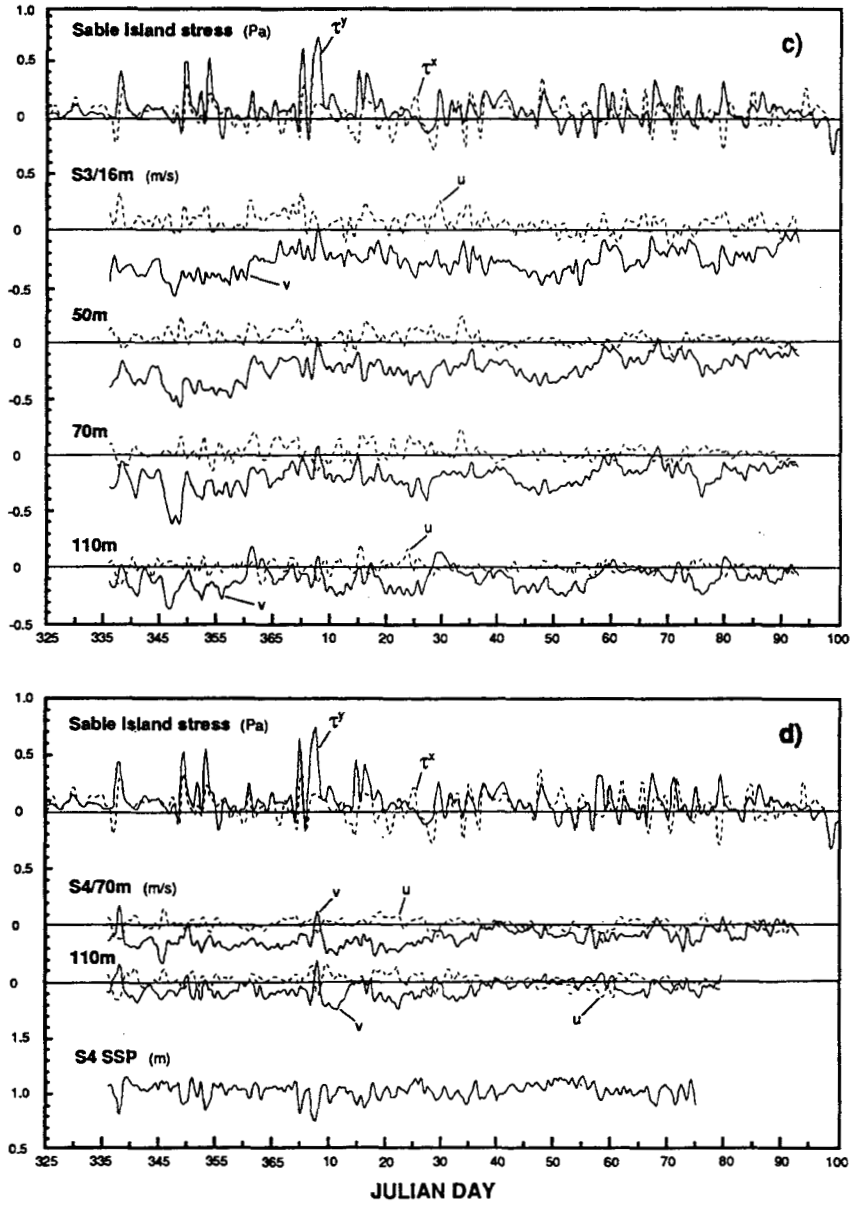

FIG. 3. (*Continued*) series are included for reference. Vertical axis units are pascals for wind stress, meters per second for velocity, and meters for bottom pressure.

and SSP on the Halifax line and at Sambro, a coastal site near the array (Fig. 7b), can be separated into low-frequency (≤0.125 cpd) and synoptic (0.2–0.5 cpd) bands containing 20%–40% and 50%–65% of the variance, respectively. Alongshelf current at S1 (Fig. 7c) peaks in two bands, 0.125 and 0.438 cpd. The gap between these bands in the nearshore current spectra is deeper than that seen in the wind stress and SSP spectra, and the relative amount of current variance in the lowest frequency bands is greater. Cross-shelf current vari-

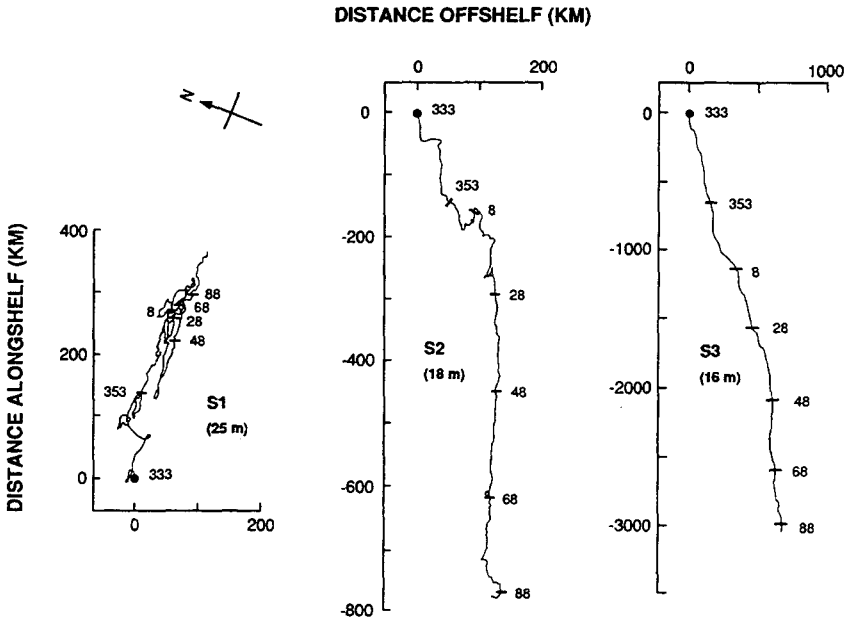

FIG. 4. Progressive vector plots comparing low-passed near-surface current records at S1 (25 m), S2 (18 m), and S3 (16 m). Tick marks denote Julian day in 1985–86. Note change in scale for S3 plot.

ance is distributed in a similar fashion, but 2–4 times less energetic at all frequencies.

At the 100-m isobath and beyond, current variance is greatly reduced at $\omega > 0.125$ cpd (Figs. 7d,e). Only at S11 (not shown) did current exhibit substantial variance at higher frequencies. Spectral variance at the lowest frequencies generally decreases seaward (cf. Figs. 7c–e) and with depth (Fig. 7d). A notable exception is S3, where variance consistently *increases* with depth at $\omega < 0.25$ cpd (Fig. 7e). With the exception of S2, where variance is noticeably reduced at all frequencies, near-surface v along the 100-m isobath displays spectra very similar to those in Fig. 7d. In general, current spectra are more "red" than those of wind stress and SSP.

Autospectral variance values in the cross-shelf component of velocity are much smaller than alongshelf variance at $\omega < 0.2$ cpd, but do not decrease as rapidly with frequency at offshore moorings. At many stations, u and v variance is nearly equal at synoptic and higher frequencies. Thus cross-shelf flow was relatively more important farther away from the coast, consistent with the magnitude of the 2–5-day oscillations in u and v noted in the time series. These results suggest that either bathymetric steering is minimal at deeper stations (i.e., bottom friction is less important, and other processes may control the circulation) or the coastline does not properly represent the local along-isobath orientation in the offshore region.

4. Statistical model

The response of SSP to meteorological forcing was estimated by Schwing (1989) using a hierarchy of multiple linear regression models in the frequency (ω) domain (Jenkins and Watts 1968; p. 493). The model that gave both the greatest statistical correlation and the most dynamically consistent results included terms that accounted for local wind stress and nonlocally forced contributions to SSP. Therefore, the response of current to meteorological forcing is described using the model

$$V(\omega) = \alpha T^y(\omega) + \beta T^x(\omega) + \gamma S^{NL}(\omega) + \epsilon(\omega). \quad (1)$$

The variables V, T^y, T^x, and S^{NL} in (1) define Fourier transforms of v, τ^y, τ^x, and SSP^{NL}, respectively, where SSP^{NL}, approximated by SSP at Louisbourg on the eastern edge of the province (Fig. 1), is a representation of the nonlocally forced contribution to SSP. The coefficients α, β, and γ are complex transfer functions and ϵ is the residual error associated with each model. Least-squares estimates of α, β, and γ give the amplitude ($|\alpha|$, $|\beta|$, $|\gamma|$) and phase (ϕ_α, ϕ_β, ϕ_γ) of the SSP response to each individual forcing term as well as the multiple coherence squared (R^2) due to the model for each frequency band centered at ω.

The determination of the least-squares estimates of the response functions uses the partial cross spectrum, which takes into account the cross-spectral relationship

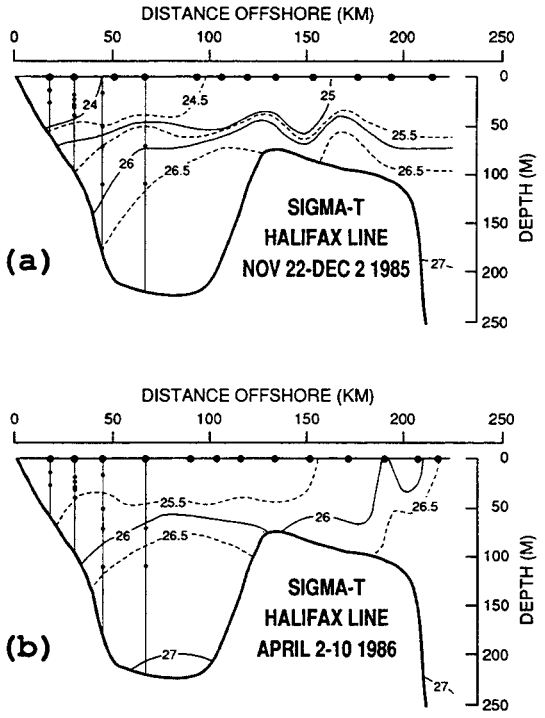

FIG. 5. Vertical density structure for a cross-shelf line extending through the Halifax current meter mooring line for (a) 22 Nov–2 Dec 1985 and (b) 2–10 Apr 1986. Current meter positions denoted by small circles on vertical lines. Larger circles denote location of hydrographic stations. Adapted from Lively (1988).

between the three independent variables (Jenkins and Watts 1968; pp. 485–487). For example, the response of current to nonlocal forcing is based on the dependence of v on SSP^{NL} *after* the effects of local wind stress (τ^y and τ^x) on the flow have been considered. This eliminates concern that the response of the dependent variable to any independent variable may be biased because the forcing terms are highly coherent. Garrett and Toulany (1982) provide further details of this technique.

Further analysis of the velocity response will focus on the alongshelf current component because it contains a majority of the low-frequency variance, and because results of the cross-shelf current analysis are statistically insignificant in most cases. Figures 8–10 summarize the response of v to SSP^{NL}, τ^y, and τ^x, the three forcing terms in the statistical model (1), at 0.125, 0.438, and 0.625 cpd. These complicated figures require a thorough orientation before the statistical results are described. Each figure presents a series of Argand, or phasor, diagrams for stations along the Halifax line [part (a) of each figure] and along the 100-m isobath [part (b)]. Each vector represents the amplitude and phase of the current response (referenced to the enclosed compass rose) to the three forcing terms at each current meter. The origin of each set of vectors is referenced to the distance scale at the top of each figure.

Bold vectors, with instrument depth shown near the arrow in large type, denote transfer functions whose amplitudes are significantly different from zero at the 0.05 level; lighter vectors with smaller-type depths are not significant. Amplitude is expressed in m s^{-1}/Pa for τ^y and τ^x, and m s^{-1}/m for SSP^{NL} forcing. Positive phase denotes current leads forcing. Vectors that rotate in a clockwise manner along a certain direction imply a phase propagation in that direction.

For example, consider the response at S1 to SSP^{NL} at 0.125 cpd (top row, left in Fig. 8a). The SSP variations (denoted by P) lag SSP^{NL} by 13°, and change 0.66 m for every 1-m change in SSP^{NL}. The alongshelf velocity at 25 m lags SSP^{NL} by 180° (i.e., flow is maximum to the west when SSP^{NL} is at its maximum) and changes by about 1.6 m s^{-1} for every 1-m change in SSP^{NL}. The gain of v at 12 m to nonlocal forcing is 1.4 m s^{-1}/m; v at 12 m lags the current at 25 m by 18°.

Figure 11 presents a series of histograms representing the alongshelf velocity variance preserved at each instrument, whose depth is given below the bar. Each is divided into four regions that represent the percentage of variance accounted for by each independent variable and a residual. The magnitude of each portion is the product of the current variance, total coherence squared (R^2), and the partial coherence between current and that forcing term, divided by the sum of the partial coherences. The R^2 value is given above the bar; all are significant to the 99% level. The responses of SSP at each mooring due to SSP^{NL}, τ^y, and τ^x (denoted by P), discussed in detail in Schwing (1989), are included in Figs. 8–11 for reference.

The selection of Louisbourg SSP as a representation of nonlocal forcing is somewhat arbitrary. It is based on the concept suggested by Gill and Schumann (1974), and others, that shelf motions at any point can be linearly separated into local (v^L) and nonlocal (v^{NL}) contributions:

$$v(x, y, t) = v^L(x, y, t) + v^{NL}(x, y, t).$$

For the Scotian Shelf, the term v^L defines the locally forced influence; that is, the velocity response to wind stress over the Scotian Shelf. That portion of v whose source lies beyond the Scotian Shelf is defined by v^{NL}, and represented by Louisbourg SSP. Results consistent with the dynamical model of Schwing (1989) indicate that the response of Louisbourg SSP to Sable Island wind stress is small at synoptic and lower frequencies, suggesting that the SSP signal there contains a significant amount of energy originating from a distant source. The anomalous autospectrum at Louisbourg (Fig. 7b) indicates this is true at higher frequencies as well. Finally, its location adjacent to the Cabot Strait makes Louisbourg SSP a good diagnostic of energy

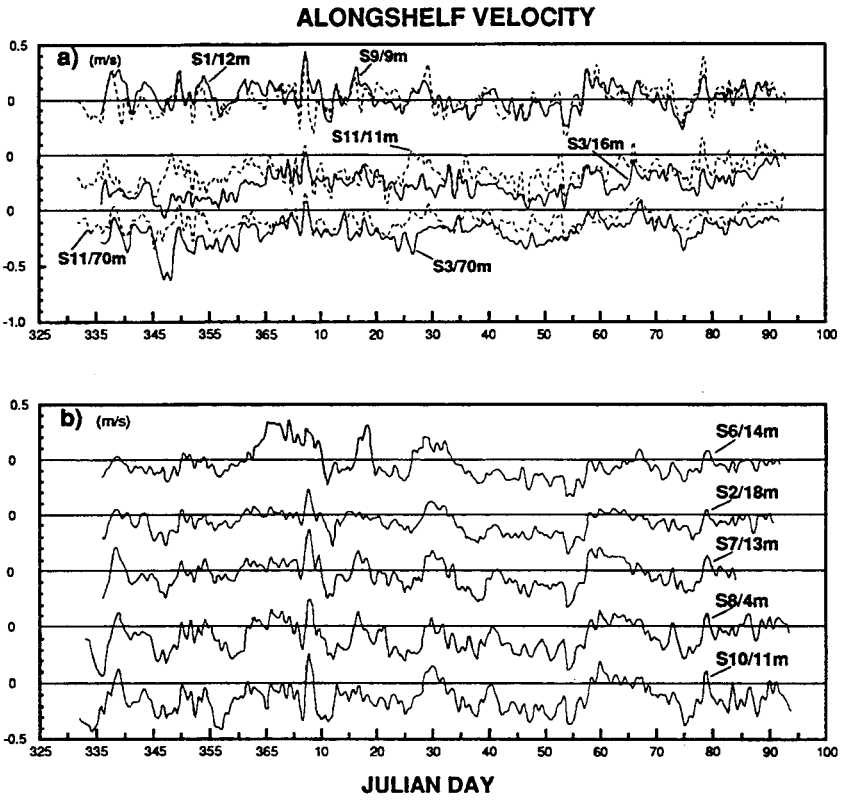

FIG. 6. Low-pass filtered time series comparing alongshelf current components at various stations in the array. (a) Comparison between S1 (12 m) (solid line) and S9 (9 m) (broken line), and between S3 (16 and 70 m) (solid lines) and S11 (11 and 70 m) (broken lines). Vertical axis units are meters per second. (b) Comparison of alongshelf current components along 100-m isobath at S6 (14 m), S2 (18 m), S7 (13 m), S8 (4 m), and S10 (11 m).

crossing the Laurentian Channel or propagating out of the Gulf of St. Lawrence. The separation of velocity into local and remote contributions will be applied further in the accompanying modeling study (Schwing 1992).

a. $\omega = 0.125$ cpd

Except for the deepest mooring S4, the alongshelf velocity field at $\omega < 0.2$ cpd, represented by the results at 0.125 cpd, is dominated by nonlocal forcing, both in terms of the response amplitude $|\gamma|$ (Fig. 8) and the percentage of variance attributed to SSP^{NL} (Fig. 11). Values of $|\gamma|$ are typically 1.0–1.5 m s^{-1}/m and decrease to the west by ~25% over an alongshelf distance of ~120 km (Fig. 8b). The cross-shelf decrease in $|\gamma|$ is much larger, about 25% between S1 and S3 (~30 km), and a factor of nearly 5 at the deepest mooring (Fig. 8a).

The phase ϕ_γ is about 180° in the nearshore region, implying that a maximum velocity to the east (west) occurs when Louisbourg SSP is at a minimum (maximum). Assuming small fluctuations in sea level at the shelf break, the nearshore alongshelf velocity is qualitatively consistent with a geostrophic balance by η_x, the cross-shelf pressure gradient. The response of SSP also implies this. The results also suggest an offshore phase propagation in the Halifax line, such that v at S3 is nearly in quadrature with SSP^{NL}. Here an eastward (westward) flow coincides with a rising (falling) SSP signal. Thus, it appears that friction dominates at shallow stations, but weakens offshore.

With the exception of S8, remotely forced currents display a consistent decrease in phase to the west, in the direction that free CTWs propagate (Fig. 8b). The phase speed over this distance is estimated to be 2–4 m s^{-1}, comparable to a second-mode CTW phase speed of 2.5 m s^{-1} calculated for the Scotian Shelf from the coastal SSP data (Schwing 1989). However, the mooring array size was small relative to the free wavelength, and confidence limits are sufficiently large such

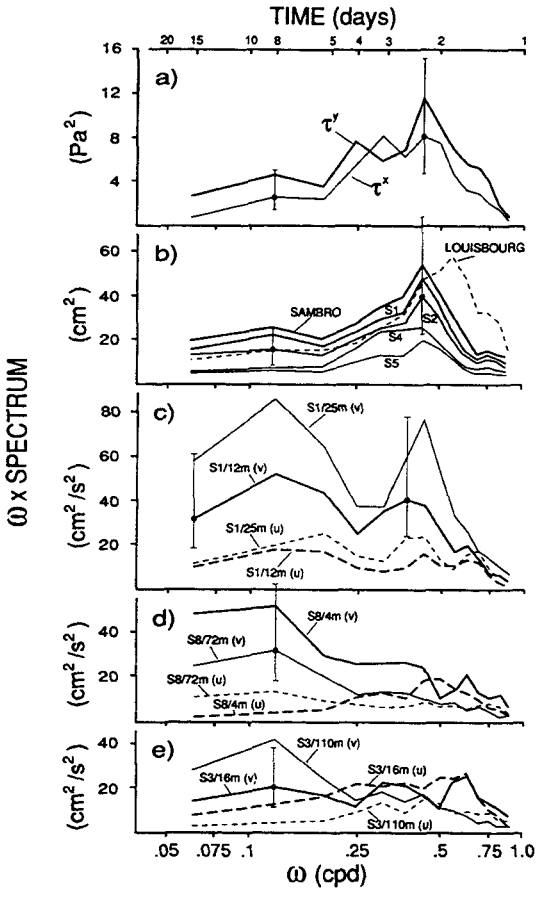

FIG. 7. Power spectra (variance preserved) of low-pass filtered time series for (a) Sable Island alongshelf (τ^y) and cross-shelf (τ^x) wind stress, (b) bottom pressure (SSP) from Halifax line (S1–S4) and coastal stations at Sambro and Louisbourg, and current components at (c) S1, (d) S8, and (e) S3. Representative 95% confidence intervals are shown.

that phase is not statistically different between stations. An array with a greater alongshelf extent is required to resolve with confidence the phase speed of the current response to nonlocal as well as local forcing.

The gains of v to local wind stress forcing ($|\alpha|$ and $|\beta|$) at 0.125 cpd are typically 0.25–0.50 m s^{-1}/Pa, but most are not significantly different from zero due to low coherence between wind stress and current. At most locations v lags τ^y by about 45° and τ^x by 120°–140° (where $|\beta|$ is significant), consistent with the cyclonic rotation of wind stress during the passage of an atmospheric low to the south of the array. The most significant features in the local wind-forced response are the generally small gains and the lack of any consistent pattern from station to station. Note particularly the anomalously small response at S2, consistent with the reduced variance observed there, as well as the relatively large response to τ^y at S7 and τ^x at S6, the westernmost mooring. These results all suggest that mesoscale variability on horizontal scales of 10–100 km is substantial in the current field, despite the absence of such variability in the SSP signal.

The velocity response to local and nonlocal forcing is uniform with depth at all stations except S3 and S7. The phase of velocity relative to SSP^{NL} and τ^x at 110 m at S3 leads the current above it by ~50°, consistent with theoretical estimates of the vertical phase shift associated with baroclinic instability (P. C. Smith, personal communication).

Finally, consider the percentage of current variance due to each independent variable, as shown in the histograms in Fig. 11. Nonlocal forcing contributes 50%–80% of the explained variance; τ^y generally accounts for much more variance than τ^x, and tends to be more important where the role of SSP^{NL} is diminished. However, the percentage due to τ^x is similar to or greater than that for τ^y in some cases (e.g., S8, S10). Thus, unlike the marginal SSP response to τ^x, the effect of cross-shelf wind stress on the current cannot be ignored. Total variance squared at 0.125 cpd varied between 0.5 and 0.8, smaller than the typical $R^2 = 0.95$ for SSP data.

The actual velocity amplitude contributed by each forcing term can be compared by estimating the amplitude of SSP^{NL}, τ^y, and τ^x from the spectral variance of each, then multiplying by the associated gain. For typical values of $|\alpha|$, $|\beta|$, and $|\gamma|$, the amplitude of the alongshelf current forced by τ^y is 1–2.5 cm s^{-1}, slightly less for τ^x, and 3–5 cm s^{-1} due to SSP^{NL}. Thus, local wind stress forcing is of secondary importance to the nonlocal contribution at low frequencies. Although $|\beta|$ values are similar to $|\alpha|$, recall that τ^y variance is 2–3 times greater in most frequency bands (Fig. 7a). Thus, the actual role of alongshelf wind stress forcing is greater. In addition, τ^y is typically more strongly correlated with v, so confidence intervals are generally larger for $|\beta|$ than $|\alpha|$.

b. ω = 0.438 cpd

The most striking change in the current response at higher frequencies ($\omega > 0.2$ cpd) is the greatly reduced response to SSP^{NL}. Values of $|\gamma|$ at 0.438 cpd are 0.25–0.50 m s^{-1}/Pa, and generally decreases offshore (Fig. 9a) and to the west (Fig. 9b). As noted at 0.125 cpd, ϕ_γ is about 180°. A geostrophic balance with the remote SSP response is again suggested. No trend in phase speed is apparent.

The magnitudes of the τ^y responses at 0.125 and 0.438 cpd are similar on and inside the 100-m isobath. However, responses at offshore stations are weaker at 0.438 cpd (e.g., S3, S4, S7). Here v lags τ^y by about 8 h at S1, with an increased lag away from the coast (Fig. 9a); $|\alpha|$ also decreases sharply offshore. In contrast,

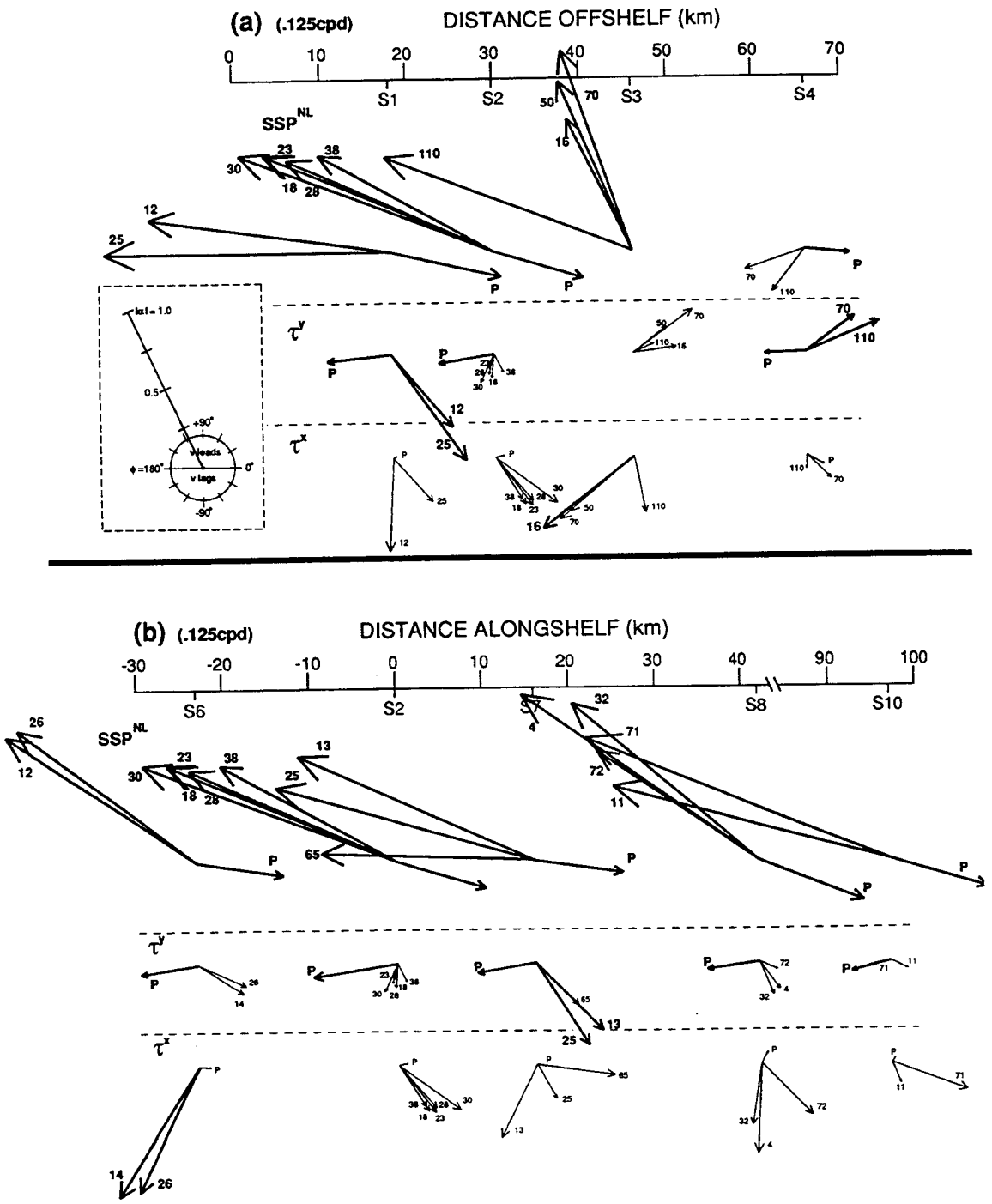

FIG. 8. Response of low-passed alongshelf current at 0.125 cpd to the forcing terms SSP^{NL}, τ^y, and τ^x in the statistical model (1) for stations in the (a) Halifax line and (b) 100-m isobath line. Vectors describe amplitude and phase of response (bold vectors and depth values denote 95% significance). SSP results from Schwing (1989), denoted by *P*, included for reference. Refer to text for further details.

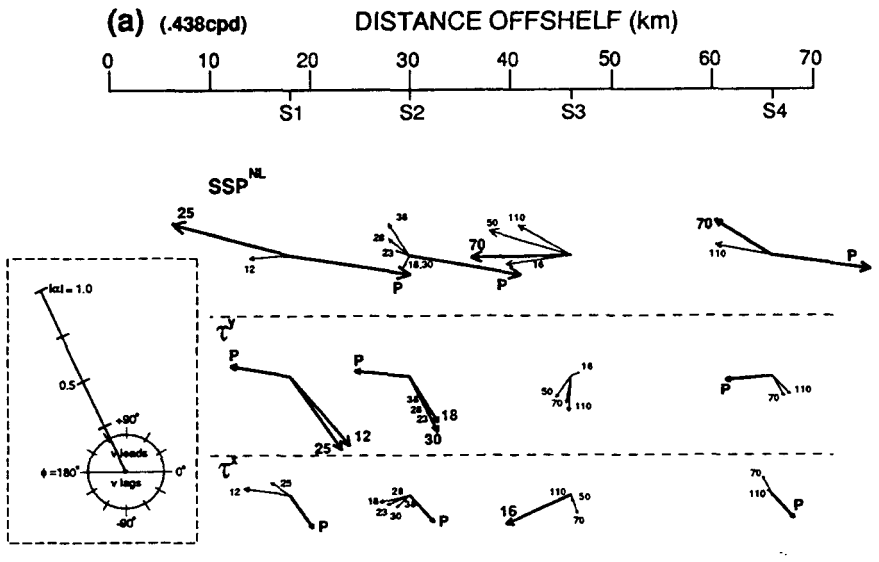

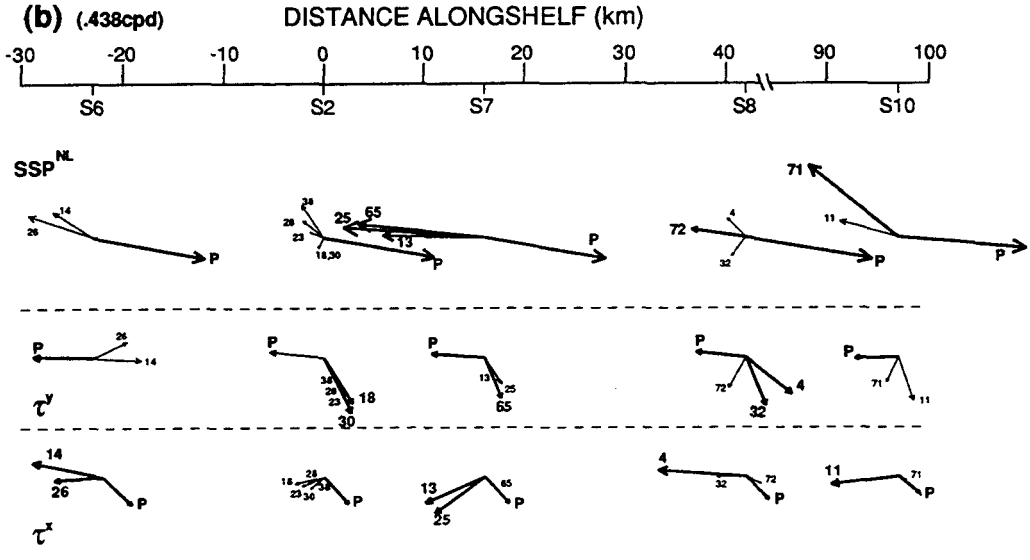

FIG. 9. Response of low-passed alongshelf current at 0.438 cpd to the forcing terms SSP^{NL}, τ^y, and τ^x in the statistical model (1) for stations in the (a) Halifax line and (b) 100-m isobath line. Vectors describe amplitude and phase of response (bold vectors and depth values denote 95% significance). SSP results from Schwing (1989), denoted by *P*, included for reference.

little consistent change in $|\alpha|$ or ϕ_α along the 100-m isobath is observed (Fig. 9b).

The response amplitude to τ^x in the surface layer is typically 0.3 m s^{-1}/Pa. Little response of v to cross-shelf wind stress is seen at depths greater than 50 m. Wright et al. (1986) observed this pattern off south-

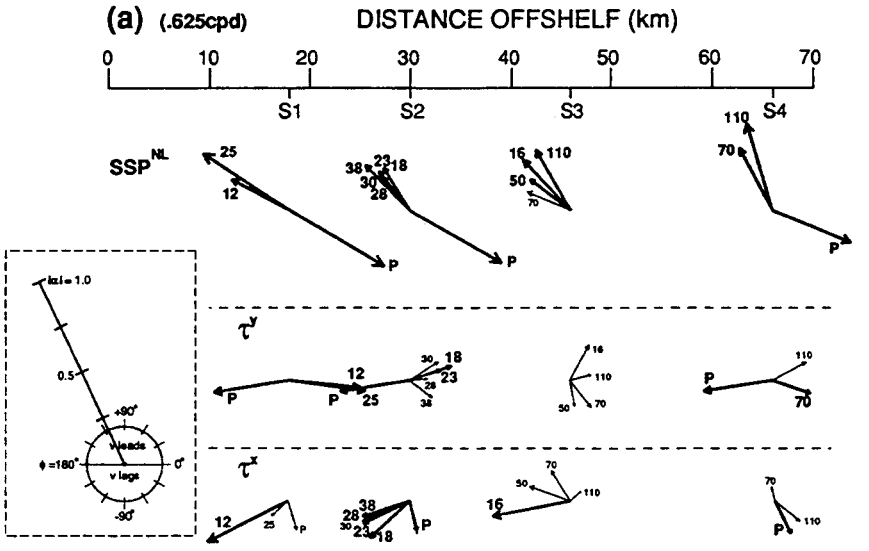

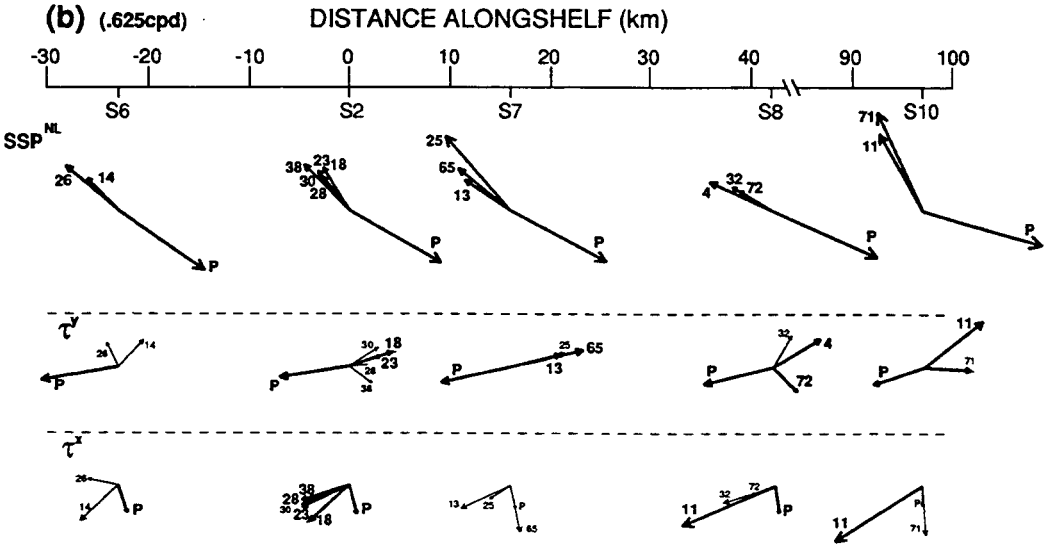

FIG. 10. Response of low-passed alongshelf current at 0.625 cpd to the forcing terms SSP^{NL}, τ^y, and τ^x in the statistical model (1) for stations in the (a) Halifax line and (b) 100-m isobath line. Vectors describe amplitude and phase of response (bold vectors and depth values denote 95% significance). SSP results from Schwing (1989), denoted by P, included for reference.

western Nova Scotia as well. Near-surface v is approximately out of phase with τ^x, consistent with a flow to the west (east) due to an offshore (onshore) wind stress.

As with the transfer functions, the dominant feature in R^2 and percent variance results is the lack of any defined trend (Fig. 11). In contrast to nearly constant

R^2 values for SSP at all frequencies, R^2 values at 0.438 cpd relative to 0.125 cpd vary greatly by station. Here R^2 appears to be related directly to the contribution from remote forcing, which accounts for a maximum of 50% but typically less than 25% of v variance. These results also suggest the reduced role of SSP^{NL} in the synoptic band. The percentage attributed to τ^y decreases noticeably with distance offshore but remains constant alongshelf.

The contribution of τ^x, however, varies greatly from station to station and decreases with depth. Stations where the response to τ^x is greatest, also where an anomalous amount of variance is explained by cross-shelf wind stress (S3, S8, S10), were located in the axis of the Nova Scotia Current (Anderson and Smith 1989). This trend is also seen at higher frequencies. Thus, variations in the intensity or position of this current at these frequencies may be controlled by τ^x.

The amplitudes of v contributed by local and nonlocal effects are more comparable than those seen at lower frequencies, primarily because the nonlocal gain is reduced by a factor of 3 or more in the synoptic band. The magnitude of the nonlocally forced alongshelf current is ~0.6–1.3 cm s^{-1}, versus ~1–2 cm s^{-1} for τ^y and ~1 cm s^{-1} for τ^x.

c. ω = 0.625 cpd

Responses at frequencies higher than the synoptic band, as exemplified by the results at 0.625 cpd (Fig. 10), are very similar in magnitude to those at 0.438 cpd. The $|\gamma|$ values are 0.25–0.50 m s^{-1}/m and exhibit little cross-shelf change (Fig. 10a), but tend to decrease to the west (Fig. 10b). The phase lead of v over SSP^{NL} decreases with distance offshore. Again the phase of the SSP response is consistent with a strongly frictional, geostrophic balance between v and η_x.

Unlike the lagged response of v to τ^y observed at lower frequencies, statistically significant ϕ_α values in the surface layer at 0.625 cpd are close to 0°. Thus, at sufficiently high frequencies the alongshelf wind-forced response appears to be frictionally dominated. Here v lags τ^x by 150°–160°, similar to 0.438 cpd, such that alongshelf current leads cross-shelf wind stress by 2–3 h. Again there is some evidence of a decrease in $|\beta|$ with depth.

The R^2 values are of similar range (0.4–0.8) as those at other frequencies, and again are smaller than associated coherences in the SSP signal (Fig. 11). In general, the importance of nonlocal forcing is smaller at higher frequencies, while the role of τ^x seems to be greater in, but confined to, the near-surface layer.

Because the variance of Louisbourg SSP does not drop off at $\omega > 0.5$ cpd, while wind stress variance is greatly reduced at these frequencies (Fig. 7b), the ratio of the remote to local current at 0.625 cpd is large relative to the synoptic band. The amplitude of v associated with SSP^{NL} and τ^y is about 0.6–1.2 cm s^{-1}, compared to the τ^x contribution of 0.5–0.9 cm s^{-1}.

5. Discussion

As discussed in the Introduction, Scotian Shelf SSP is effectively accounted for by a statistical model that includes local and remote forcing (Schwing 1989). The response of the pressure field to wind stress and nonlocal effects is also physically meaningful. These features stand in contrast to the subinertial current response described previously, with its reduced correlations and sizable variability from station to station. Some patterns in the velocity response are reflected in the SSP behavior. Alternatively, the relatively poor statistical results and differences between the v and SSP responses suggest additional dynamical processes that may profoundly influence circulation, yet are unaccounted for by simple dynamical models, such as those applied by Csanady (1978) and Schwing (1989).

The most obvious similarity between alongshelf velocity and SSP is in their remotely forced (free) contributions. The amplitudes of the response of both parameters typically decay to the west and offshore. Changes in phase generally imply a propagation to the west, consistent with the direction of freely propagating CTWs. However, the phase speed in the velocity signal is difficult to determine with statistical certainty, given the generally large confidence intervals and the relatively small spatial extent of the mooring array.

A comparison of the v and SSP responses to remote forcing at any mooring reveals that the two signals are approximately out of phase at all frequencies (Figs. 8–10). A simple geostrophic balance gives the alongshelf barotropic transport through the Halifax line provided

$$\Delta\eta = \frac{f}{g}\int_0^{x=S5} \bar{v}\,dx, \qquad (2)$$

where $\Delta\eta$ is the difference between the nonlocal SSP response at S5 and Sambro (at the coast), and $\bar{v}$ is the depth-averaged alongshelf current response for the significant results presented in Figs. 8–10. A comparison of $\Delta\eta$ to $\widehat{\Delta\eta}$, an estimate of the cross-shelf pressure gradient based on the averaged current gain at S1–S4 [rhs of (2)] demonstrates that the remote response is primarily geostrophic (Table 1). The estimate of the cross-shelf pressure gradient is poorest at 0.125 cpd.

A geostrophic balance between the local wind-forced current and SSP is tested as well. Applying (2) to the τ^y response suggests the wind-forced alongshelf current is balanced by the pressure gradient at $\omega > 0.2$ cpd. Like the remote response, however, transport at the lowest frequencies overestimates the gradient. Thus, quasi-steady motions appear to involve a more complex set of dynamics.

The data described here are consistent with other results suggesting that the Scotian Shelf response is largely wind driven (Petrie and Smith 1977; Smith et al. 1978; Sandstrom 1980; Schwing 1989). A comparable set of response functions was determined from velocity records obtained off southwestern Nova Scotia,

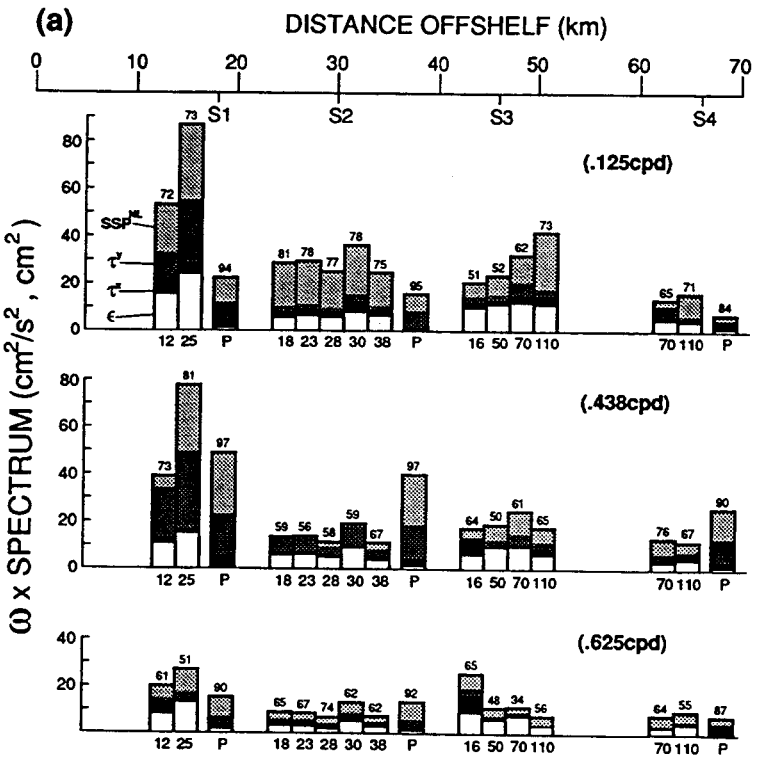
(a)
DISTANCE OFFSHELF (km)
0 10 20 30 40 50 60 70
S1 S2 S3 S4
(.125cpd)
(.438cpd)
(.625cpd)
ω x SPECTRUM (cm²/s², cm²)
SSP^ML
τ^v
τ^w
ε
12 25 P 18 23 28 30 38 P 16 50 70 110 70 110 P

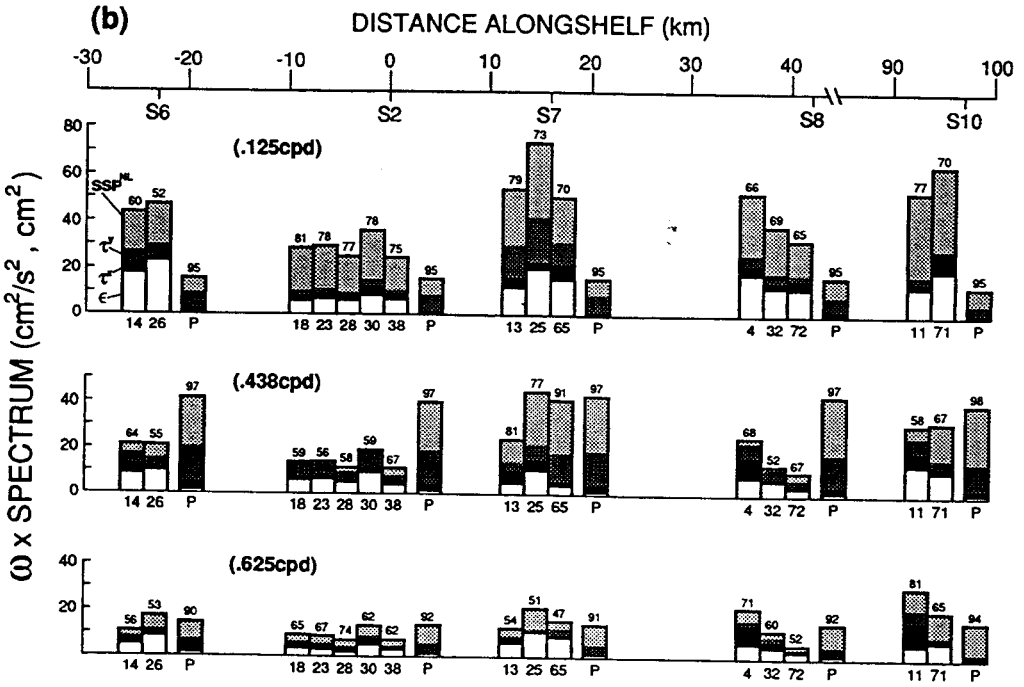
(b)
DISTANCE ALONGSHELF (km)
-30 -20 -10 0 10 20 30 40 90 100
S6 S2 S7 S8 S10
(.125cpd)
(.438cpd)
(.625cpd)
ω x SPECTRUM (cm²/s², cm²)
SSP^ML
τ^v
τ^w
ε
14 26 P 18 23 28 30 38 P 13 25 65 P 4 32 72 P 11 71 P

west of the CASP array (Wright et al. 1986). Quasi-steady alongshelf current gains to alongshelf wind stress at Sable Island are 0.5–0.75 m s^{-1}/Pa, based on three moorings inside the 100-m isobath. This response is very similar to that seen at S1 at 0.125 cpd (Fig. 8a). The amplitudes of the nearshore current responses are also reasonably consistent with the steady numerical model results of Wright et al. Preliminary analysis of the current observations off southwest Nova Scotia, using the multiple regression model applied to the CASP records, has given results consistent with the locally and remotely forced time-dependent results described here (P. C. Smith, personal communication).

Wright et al. (1986) also clearly demonstrate the importance of a properly prescribed sea level condition at the backward (eastern) boundary of their model. A setup in coastal pressure at that boundary, which presumably represents the effect of wind stress integrated over the backward portion of the shelf, is required to properly estimate the observed current gains. This setup can be thought of as the remote contribution to the total flow, consistent with the statistical approach used here. The SSP and current gains calculated in the previous section also suggest that the magnitude of the coastal setup applied by Wright et al. is reasonable.

The importance of cross-shelf wind stress forcing of v during CASP was confined near the surface, particularly in the synoptic band. Wright et al. (1986) observed a similar pattern. Such results suggest that contributions from τ^x are primarily in the form of a near-surface (possibly Ekman) flux alongshelf, somewhat reduced relative to the alongshelf flow due to τ^y. A similar relationship between τ^y and u may exist. However, nearly all cross-shelf current responses are too small to be presented with statistical certainty. Cross-shelf flux time series are neither visually nor statistically coherent.

Features of the meteorologically forced circulation of the Scotian Shelf are also consistent with observations from adjacent shelf areas. Flow on the Labrador (Webster and Narayanan 1988) and Newfoundland (Greenberg and Petrie 1988) shelves is generally parabathic, but also features substantial mesoscale variability. Wright et al. (1987) and Webster and Narayanan (1988) conclude that nonlocal forcing, probably originating from Hudson Bay, is a major contributor to the flow. Noble et al. (1983) found 75%–90% of low-frequency alongshelf current variance on Georges Bank and in the Middle Atlantic Bight, west of the Scotian Shelf, is due to the combined effects of local wind forcing and free propagations. Ou et al. (1981) reached a similar conclusion for the Middle Atlantic Bight. The relative contribution of these sources of variability varies with location; remote forcing is relatively more important on Georges Bank. Thus, the idea of separating the circulation into local and remote portions is valid in regions adjacent to the Scotian Shelf.

TABLE 1. A comparison of the cross-shelf difference in the amplitude of the SSP response to SSP^{NL} and τ^y. The terms $\Delta\eta$ are the differences in the response of SSP at Sambro and S5 (taken from Schwing 1989) for three representative frequency bands. $\widehat{\Delta\eta}$ values are estimates of this difference found by integrating the appropriate depth-averaged alongshelf current responses at S1–S4, based on the geostrophic balance $\eta_x = (f/g)v$.

	Nonlocal (SSP^{NL}) (m s^{-1}/m)		Local (τ^y) (m s^{-1}/Pa)	
ω(cpd)	$\Delta\eta$	$\widehat{\Delta\eta}$	$\Delta\eta$	$\widehat{\Delta\eta}$
.125	.55	.85	.19	.34
.438	.25	.27	.20	.21
.625	.30	.31	.24	.20

The discrepancy between the spatial coherence scales of SSP and current described here is similar to the results of Vermersch et al. (1979) for the Gulf of Maine. While the winter pressure field is highly coherent over the entire gulf, the horizontal coherence scale of the velocity field is less than 50 km and current is poorly correlated with local wind. Vermersch et al. speculate that the gulf's very rough bathymetry is responsible for generating mesoscale eddies. The results of Webster and Narayanan (1988) suggest that bathymetric irregularities also lead to significant variations in flow on the Labrador Shelf. The dominant bathymetric scales of these two regions are quite similar to those of the CASP study area; thus, the idea of bathymetrically influenced flow on the Scotian Shelf is worth considering and is pursued in the numerical study that follows (Schwing 1992).

Because the wind-forced responses observed in this study are small and associated confidence intervals are large, it is difficult to estimate the phase speed at which locally forced features propagate through the current array. However, the strongest response to τ^y (at 0.438 cpd) suggests an alongshelf phase propagation to the west, consistent with the SSP response. Thus, gross features of the forced and free current response can be accounted for by similar physically intuitive models (cf. Csanady 1978; Schwing 1989). However, mesoscale variations in the velocity field that do not appear in the SSP signals must develop in response to either 1) a more complex set of physics or 2) a complex bathymetry or wind field that does not affect pressure to nearly the same degree.

FIG. 11. (a) Percentage of low-passed alongshelf current variance due to each of the forcing terms (SSP^{NL}, τ^y, and τ^x), and model error in the statistical model (1), for stations in the (a) Halifax line and (b) 100-m isobath line. Height of each histogram bar denotes total current variance (variance preserved) at the depth given below each bar. Total percentage of variance explained by the model given above each bar. SSP results from Schwing (1989), denoted by P, included for reference.

Current observations typically are associated with smaller dominant length scales than are SSP observations (cf. Rhines 1977, pp. 196–202). Willebrand et al. (1980) have shown that spatial inhomogeneities in wind or bathymetry can cause wind and current signals to become incoherent. The SSP can be thought of as an integral measure of the flow. Thus, it is analogous to a spatially filtered representation of the circulation, in which variations due to wind stress or bathymetry on subsynoptic horizontal scales are removed. For a spatially uniform wind or bathymetry, the velocity field is fairly homogeneous and would be changed little by this "filtering" process; thus, velocity and SSP coherence scales are similar. However, as the dominant scales for wind stress or bathymetry decrease, so do those for the circulation. In the case of a spatially complex depth or wind field, pressure—the integral representation of the flow—is strongly incoherent with velocity.

Finally, it is important to note that the horizontal extent of the CASP instrument array was small relative to those of wind-forced and free circulation features. These small distances, and the relatively large confidence intervals, point to the need for a spatially more extensive current meter and bottom pressure array to confidently replicate the scales of the locally and nonlocally forced responses detected in the coastal SSP records (Schwing 1989). The ongoing analysis of current meter records obtained over the western portion of the Scotian Shelf, off West Head (Fig. 1), using the multiple regression model applied here (P. C. Smith, personal communication) will hopefully shed some light on this issue.

6. Summary

Two primary current regimes exist on the portion of the Scotian Shelf covered by the CASP mooring array. Flow inside the 100-m isobath is rectilinear and parallel to the general bathymetry. Although the record mean is nearly zero, the predominantly alongshelf current oscillates at periods of 2–5 d in response to local wind forcing over the shelf. Maximum velocities of 0.2–0.3 m s^{-1} were recorded in this nearshore region. The current at offshore moorings features a mean westward velocity of about 0.3 m s^{-1}, although a meteorological response at synoptic frequencies is again observed. The time-varying portion of velocity in both regions is generally uniform with depth. Anderson and Smith (1989) conclude that the mean circulation during CASP was predominantly barotropic. The results of Lively (1988) suggest the flow is largely barotropic at synoptic periods as well, particularly in the near-surface layer and throughout the inner portion of the shelf. However, the potential importance of baroclinicity cannot be completely ignored on the outer shelf.

In contrast to the highly coherent response of SSP to local and remote forcing, the velocity response, obtained with a multiple regression model that includes local and nonlocal effects, exhibits substantial variability from station to station, and is not nearly as coherent with wind stress. Nonlocal forcing dominates at $\omega < 0.2$ cpd, while local wind and remote contributions are similar at higher frequencies. Cross-shelf forcing has more effect on current than SSP, but its influence is limited to the near-surface layer. The total velocity variance explained with this model is about 40%–80%, and is generally highest at the shallow stations.

Both velocity components exhibit regions of flow that are poorly correlated with local and remote forcing, vary without pattern in space, and are generally inconsistent with SSP results. If averaged over the mooring array, the statistical results suggest that many of the current patterns are also observed in SSP data, and can be related to physically meaningful concepts. For example, CTW activity is suggested by characteristics of the velocity and SSP response to remote forcing. The current response to local and remote forcing integrated across the Halifax line is consistent with the geostrophic flow estimated from the SSP response; thus, the large-scale current can be determined from the pressure field. However, velocity variations on scales of 10–100 km are not reflected in the SSP signal, which implies that the rugged bathymetry of the Scotian Shelf may induce modifications in the circulation that are not manifested in the SSP records.

In a companion paper (Schwing 1992), a numerical model is developed and applied to the problem of wind-forced flow over irregular bathymetry. Two particular questions will be explored. First, how and to what degree do bathymetric variations, like those seen on the Scotian Shelf, influence locally and remotely forced circulation patterns? Second, how are these perturbations reflected differently in SSP and velocity? It is hoped that model results will explain the discrepancies between the highly coherent SSP response and the irregular velocity response, as detailed here.

Acknowledgments. I am grateful to Drs. Keith Thompson, Peter Smith, Dan Wright, Chris Garrett, and Ken Brink for their stimulating scientific discussion and critical review during the preparation of this manuscript. I also acknowledge the scientific and logistic support of many individuals at Bedford Institute of Oceanography, particularly Dr. Carl Anderson. This work was supported (in part) by the Federal Panel on Energy R&D (PERD).

REFERENCES

Anderson, C., and P. C. Smith, 1989: Oceanographic observations on the Scotian Shelf during CASP. *Atmos.–Ocean*, **27**, 130–156.

——, F. Dobson, W. Perrie, F. Schwing, P. Smith, and B. Toulany, 1989: Storm response in the coastal ocean: The oceanographic component of the Canadian Atlantic Storm Program (CASP). *Trans. Amer. Geophys. Union*, **70**(18), 562–572.

Carter, G. C., and J. F. Ferrie, 1979: A coherence and cross-spectral estimation program. *Programs for Digital Signal Processing,*

Edited by the Digital Signal Processing Committee, 2.3.1–2.3.18, IEEE Acoustics, Speech and Signal Processing Society, The Institute of Electrical and Electronic Engineers.

Csanady, G. T., 1978: The arrested topographic wave. *J. Phys. Oceanogr.*, **8**, 47–62.

Drinkwater, K. F., and G. B. Taylor, 1982: Monthly means of temperature, salinity and density along the Halifax Section. Tech. Rep. of Fish and Aquatic Sci., No. 1093, 67 pp.

——, B. Petrie, and W. H. Sutcliffe, Jr., 1979: Seasonal geostrophic volume transports along the Scotian Shelf. *Estuarine Coastal Mar. Sci.*, **9**, 17–27.

Garrett, C., and B. Toulany, 1982: Sea level variability due to meteorological forcing in the northeast Gulf of St. Lawrence. *J. Geophys. Res.*, **87**, 1968–1978.

Gill, A. E., and E. H. Schumann, 1974: The generation of long shelf waves by the wind. *J. Phys. Oceanogr.*, **4**, 83–90.

Greenberg, D. A., and B. D. Petrie, 1988: The mean barotropic circulation on the Newfoundland shelf and slope. *J. Geophys. Res.*, **93**, 15 541–15 550.

Haidvogel, D. B., and K. H. Brink, 1986: Mean currents driven by topographic drag over the continental shelf and slope. *J. Phys. Oceanogr.*, **16**, 2159–2171.

Hsieh, W. W., 1982: On the detection of continental shelf waves. *J. Phys. Oceanogr.*, **12**, 414–427.

Jenkins, G. M., and D. G. Watts, 1968: *Spectral Analysis and its Applications.* Holden-Day, 525 pp.

Lewis, P. J., and M. D. Moran, 1984: Severe storms off Canada's East Coast: A catalogue summary for the period 1957 to 1983. Canadian Climate Centre, Rep. No. 84–13, Atmosphere Environmental Service, Downsview, Ontario, 345 pp.

Lively, R. R., 1988: Current Meter, Meteorological, Sea-Level and Hydrographic Observations from the CASP Experiment, off the Coast of Nova Scotia, November 1985 to April 1986. Can. Tech. Rep. Hydrogr. Ocean Sci., No. 100, vii+428 pp.

Noble, M., B. Butman, and E. Williams, 1983: On the longshore structure and dynamics of subtidal currents on the eastern United States continental shelf. *J. Phys. Oceanogr.*, **13**, 2125–2147.

Ou, H. W., R. C. Beardsley, D. Mayer, W. C. Boicourt, and B. Butman, 1981: An analysis of subtidal current fluctuations in the Middle Atlantic Bight. *J. Phys. Oceanogr.*, **11**, 1383–1392.

Petrie, B. D., and P. C. Smith, 1977: Low-frequency motions on the Scotian Shelf and Slope. *Atmosphere*, **15**, 117–140.

Rhines, P. B., 1977: The dynamics of unsteady currents. *The Sea: Ideas and Observations on Progress in the Study of the Seas, Marine Modeling*, Vol 6, Goldberg, E. D., I. N. McCave, J. J. O'Brien, and J. H. Steele, Eds., John Wiley and Sons, 189–318.

Sandstrom, H., 1980: On the wind-induced sea level changes on the Scotian Shelf. *J. Phys. Oceanogr.*, **10**, 461–468.

Schwing, F. B., 1989: Subtidal response of the Scotian Shelf bottom pressure field to meteorological forcing. *Atmos.–Ocean*, **27**, 157–180.

——, 1992: Subtidal response of the Scotian Shelf circulation to local and remote forcing. Part II: Barotropic model. *J. Phys. Oceanogr.*, **22**, 542–563.

Smith, P. C., 1989: Inertial oscillations near the coast of Nova Scotia. *Atmos.-Ocean*, **27**, 181–209.

——, B. Petrie, and C. R. Mann, 1978: Circulation, variability and dynamics on the Scotian Shelf and Slope. *J. Fish. Res. Board Can.*, **35**, 1067–1083.

Smith, S. D., and E. G. Banke, 1975: Variation of the sea surface drag coefficient with wind speed, *Quart. J. Roy. Meteor. Soc.*, **101**, 665–673.

Stewart, R. E., R. W. Shaw, and G. A. Isaac, 1987: Canadian Atlantic Storms Program: The meteorological field project. *Bull. Amer. Meteor. Soc.*, **68**, 338–345.

Vermersch, J. A., R. C. Beardsley, and W. S. Brown, 1979: Winter circulation in the western Gulf of Maine: Part 2. Current and pressure observations. *J. Phys. Oceanogr.*, **9**, 768–784.

Webster, I., and S. Narayanan, 1988: Low-frequency current variability on the Labrador Shelf. *J. Geophys. Res.*, **93**, 8163–8173.

Wilkin, J. L., and D. C. Chapman, 1987: Scattering of continental shelf waves at a discontinuity in shelf width. *J. Phys. Oceanogr.*, **17**, 713–724.

Willebrand, J., S. G. H. Philander, and R. C. Pacanowski, 1980: The oceanic response to large-scale atmospheric disturbances. *J. Phys. Oceanogr.*, **10**, 411–429.

Wright, D. G., D. A. Greenberg, J. W. Loder, and P. C. Smith, 1986: The steady-state barotropic response of the Gulf of Maine and adjacent regions to surface wind stress. *J. Phys. Oceanogr.*, **16**, 947–966.

——, ——, and F. G. Majaess, 1987: The influence of bays on adjusted sea level over adjacent shelves with application to the Labrador Shelf. *J. Geophys. Res.*, **92**, 14 610–14 620.